C1, 93 (1970).
[6]D. M. Newns, Phys. Letters 33A, 43 (1970).
[7]D. M. Newns, Phys. Rev. Letters 25, 1575 (1970).
[8]F. Ducastelle and F. Cyrot-Lackmann, J. Phys. Chem Solids 32, 285 (1971).
[9]R. E. Watson and H. Ehrenreich, Commun. Solid State Phys. 3, 109 (1970).
[10]F. Ducastelle and F. Cyrot-Lackmann, J. Phys. Chem. Solids 31, 1295 (1970).
[11]J. C. Slater and G. Koster, Phys. Rev. 94, 1498 (1954).
[12]M. Dreschler, Z. Elecktrochem. 58, 327 (1954); P. Wynblatt and N. A. Gjostein, Surface Sci. 22, 125 (1970).
[13]F. Herman and S. Skillman, *Atomic Structure Calculations* (Prentice-Hall, Englewood Cliffs, N. J., 1963).
[14]One has to notice that this value should be somewhat reduced if we were able to compute the overlap integrals in a self-consistent way.
[15]In his first computation (Ref. 6), using a virtual-bound-state model, Newns has obtained results similar to ours. But this has the same disavantage as his last approach (Ref. 7), as the cohesive energy of bulk transition metal cannot (Ref. 7) be reasonably obtained in this way.

PHYSICAL REVIEW B VOLUME 4, NUMBER 8 15 OCTOBER 1971

Generalized Locator–Coherent-Potential Approach to Binary Alloys

J. A. Blackman*† and D. M. Esterling*
Physics Department, Indiana University, Bloomington, Indiana 47401

and

N. F. Berk‡
Department of Physics and Astronomy, University of Maryland, College Park, Maryland 20742
(Received 12 March 1971; revised manuscript received 25 May 1971)

The electronic structure of binary alloys is discussed for a system in which both the atomic energy levels and the hopping integrals are random quantities. This paper is a detailed study of the generalization of the coherent-potential approximation (CPA) introduced earlier by the present authors. We show that a locator description provides a particularly suitable formalism for setting up this generalized problem and how, with the aid of a simple device, configuration averaging may be performed by the use of established techniques. The approximation used is, as in the case of the usual CPA, a single-site one. Three self-consistent equations are obtained that must be solved simultaneously; these replace the single CPA equation. Numerical results are displayed for a series of alloys, and a discussion of certain aspects of the theory, such as its moment-preserving properties, is also included.

I. INTRODUCTION

Much of the work on the electronic theory of binary alloys has been a development of the multiple-scattering formalism of Lax.[1] At present a rather satisfying stage in the theory seems to have been reached with the introduction of the coherent-potential approximation (CPA) by Soven,[2] and its subsequent developments.[3,4] The simplicity of the CPA arises from the fact that formally it can be viewed as a reduction of the alloy problem to one of a single impurity in a self-consistently determined effective lattice. In the usual tight-binding model, only the atomic energy levels are assumed to be random, i.e., to depend on the occupation of sites by either of the constituent species. In the effective-medium approach one replaces the averaged alloy by a periodic lattice of "effective atoms," whose effective localized energy is to be determined, and whose coupling (via hopping integrals) is the same as in the real alloy. One now introduces a single real atom into the effective lattice (this replacement, it is assumed, does not affect the coupling, but has only the effect of producing a perturbation localized on the impurity site itself) and determines the condition that on the average (the impurity can be either of two species) no scattering occurs, i.e., the average single-site t matrix is zero. This gives the CPA self-consistency condition.

The introduction of this effective lattice simplifies the derivation of the self-consistency equation, but it is not essential. For example, we can use, if we wish, the virtual crystal—or indeed the pure lattice of either of the constituent atomic species—as the "unperturbed" lattice, and then perform the more complicated multiple-scattering calculation. The difficulty then arises of dealing with multiple-occupancy effects correctly. This has been done by Leath,[5] among others. Using a diagrammatic propagator expansion technique, Leath shows how to sum all non-crossed-line diagrams in the perturbation series. Since such diagrams have a single-site nature, their summation

is equivalent to the CPA.

The mathematical apparatus is very similar for a variety of the elementary excitations and a body of literature now exists that, while containing variations in appearance, is equivalent to the CPA: for electrons, Soven,[3] Velický *et al.*,[4] and Yonezawa[6]; for phonons, Leath[5] and Taylor[7]; and for excitons, Onodera and Toyozawa.[8]

All of the work mentioned above adopts a propagator formalism. An alternative approach is the locator method introduced by Matsubara and Toyozawa[9] and extended by Matsubara and Kaneyoshi.[10] A summary of the technique is given in the work of Ziman.[11] The essence of the method is to use, as a starting point, localized atomic states (as opposed to the Bloch states of the propagator formalism), and to allow delocalization via the overlap (hopping) integral. In the usual alloy model it is the energy of these localized states that is the random quantity, the hopping integral being taken as independent of the nature of the pair of sites involved. The locator expansion can be represented by a set of diagrams that are equivalent topologically to those of the propagator expansion. Just as in the propagator expansion, the summation of all single-site (non-crossed-line) diagrams retrieves the CPA result, as demonstrated in the work of Leath.[12] His work thus establishes an equivalence between the two approaches at the lowest order in a cluster expansion, and is suggestive of an equivalence for higher-order clusters as well. It is worth noting here that a locator-type expansion was also used by Anderson[13] to discuss the localization problem. The development in that work was rather different, however, because of the need to determine a probability distribution rather than an average.

Several lines of development of the CPA (or equivalent theories) have suggested themselves. The inclusion of contributions from higher-order clusters (crossed-line diagrams) would be one way of improving the CPA. An attempt to include the effect of two-site clusters is described in the work of Aiyer *et al.*[14] Another line of development concerns the failure of the CPA to give a finite density of states out to the component band edges. This failure violates a requirement discussed by Lifshitz,[15] and is a particular drawback in applying the CPA to optical phenomena. Recent work by Eggarter and co-workers[16] attempts to rectify the deficiency by a moment approach in the energy region near the true band edges.

Another significant area of development has been the extension of the alloy theory to the physically important case of alloys whose pure constituents have different bandwidths. Within the tight-binding or Wannier scheme, this means removing the restriction (common to early treatments of the CPA) that the hopping integrals of the model be independent of the occupation of the sites which are coupled. The problem of a random hopping integral has been treated previously in two limiting cases. Takeno[17] (see also analogous spin-wave work of Izyumov[18]) investigated the limit of small impurity concentration, allowing the impurity potential to extend via off-diagonal matrix elements to neighboring host sites. The resulting extended impurity cluster (i.e., impurity atom plus neighboring host atoms) was then treated as the scattering entity, but with the important assumption that these impurity clusters do not overlap. Scattering within the cluster is treated exactly and, when averaging, the cluster takes the place of the single-site scatterer of the CPA or the appropriate low-concentration theory. Because nonoverlap of the potentials is essential to the approach, no parameter for impurity-impurity coupling appears in the results and there appears no obvious way of extending the theory to alloys of general composition. A second limiting case, that of weak coupling, has been discussed by Berk.[19] In this regime, both the diagonal and off-diagonal parts of the model Hamiltonian are allowed to be random, but fluctuations of the matrix elements about their average values are assumed to be sufficiently small that scattering from these fluctuations can be treated in second order of self-consistent perturbation theory. More recently, Soven[20] has recast the CPA for a system of random muffin-tin potentials. When the model is appropriate, the choice of constituent muffin-tin potentials accounts for the different bandwidths of the pure solute and solvent materials, and the theory is not limited, as such, to a particular regime of parameters.

In this paper we present another approach[21] to the problem of "off-diagonal randomness," using the Wannier representation of the model alloy Hamiltonian. The physical parameters (as in the work of Takeno and Berk) are the atomic energies and the hopping integrals (or masses and force constants in the phonon case). Like Soven's, our theory is not subject to any special limits. Recently new work has appeared by Tanaka *et al.*[22] and by Shiba.[23] The latter bears some resemblance to our approach, but (for an AB alloy) is restricted to the case of the A-B hopping being the geometric mean of the A-A and B-B hoppings.

The theory we shall describe here is expressed in a locator language and may be described as a generalization of Leath's[12] locator formalism of the CPA. The physical content of the method is described very simply. We start with a random set of basis states and allow delocalization via hopping which is also random (although correlated, of course, to the randomness of the basis states themselves). When it comes to performing con-

figuration averages, the approximation we use is, as in the CPA, of a single-site nature. Although it may not be immediately obvious that a single-site theory is possible when off-diagonal randomness is present, we will show that, in a locator formalism, its use appears very naturally.

As discussed at the beginning of this section, what is implied by a single-site type of approximation (such as the CPA or our generalization of it) is the concept of an A or B type of atom embedded in an effective environment. If one then decides to use a locator language, what one is essentially doing is considering the way an electron diffuses away from the A or B impurity; i.e., one calculates the self-energy corrections to the A or B locator. In the standard CPA (nonrandom hopping integral) the self-energy corrections are independent of the atomic species, reflecting the fact that both A and B atoms "see" the same effective environment (see Sec. III). When we introduce randomness into the hopping, however, the manner in which the electron diffuses away (and hence also the renormalization effects) will be dependent on the atomic species.

The averaging technique that we use is parallel to that of Leath.[12] It does, however, differ somewhat in procedure, and thus we present a derivation of the locator approach to the standard CPA in Sec. II, which will be appropriate for the generalizations of subsequent sections of this paper. In Sec. III we set up a locator expansion for the alloy in which randomness in the hopping is included. We also describe a device for formally associating all the randomness with single sites, thus expediting the averaging process. On averaging, a set of three self-consistent equations is obtained that must be solved simultaneously. A confirmation of a satisfactory reduction to the standard CPA in the appropriate limit is given in Sec. IV. To illustrate the behavior of the theory, numerical results for a simple cubic lattice with nearest-neighbor coupling are shown in Sec. V. Finally, in Sec. VI, we turn to more general considerations such as the moment-preserving properties of the theory.

II. LOCATOR APPROACH TO STANDARD CPA

Our purpose in this section is to discuss a procedure for obtaining the CPA in terms of a locator expansion for the usual model alloy, i.e., allowing only the diagonal part of the Hamiltonian to depend on site occupation. Leath[12] has already worked this out in detail, but we present it here since our derivation of the result is somewhat different and bears directly on the subsequent generalization.

The model Hamiltonian is

$$H=\sum_i \epsilon_i a_i^\dagger a_i+\sum_{i,j} t_{ij} a_i^\dagger a_j \ , \tag{2.1}$$

where $a_i^\dagger$ and a_i are electron creation and annihilation operators in the Wannier representation (subscripts i refer to lattice sites). t_{ij} is the hopping integral between sites i and j (for the moment assumed independent of the atomic species occupying the two sites). We take t_{ii} equal to zero. The diagonal energies ϵ_i can take values E_A or E_B depending on the type of atom occupying site i.

In the locator formalism, the alloy Green's function G satisfies the equation

$$\begin{aligned} G_{ll'} &= g_l\delta_{ll'}+g_l t_{ll''} G_{l''l'} \\ &= g_l\delta_{ll'}+g_l t_{ll'} g_{l'}+g_l t_{ll''} g_{l''} t_{l''l} g_{l'}+\cdots . \end{aligned} \tag{2.2}$$

Summation over repeated indices is understood. The symbol g denotes the bare locator which can take either of two possible values, viz., $(E-E_A)^{-1}$ or $(E-E_B)^{-1}$. The fully renormalized locator γ is defined in this work, in terms of the configurationally averaged Green's function, by

$$\gamma=\langle G_{ll}\rangle=\langle G\rangle_0 \ , \tag{2.3}$$

where the subscript zero denotes the diagonal part of the averaged G. The fully renormalized locator is thus the properly averaged sum of all terms in (2.2) which start and end on the same site. It will be noticed, at this point, that our definition of the renormalized locator differs from the usual one (e.g., Ref. 12). A comparison of the two approaches will be deferred until the end of this section. Once γ is known, the density of states of the averaged system is given by

$$\rho=-(1/\pi N)\,\mathrm{Im}\textstyle\sum_k G_k=-(1/\pi)\,\mathrm{Im}\gamma \ , \tag{2.4}$$

where G_k is the averaged alloy Green's function in the k representation.

Now let us consider specifically the single-site approximation. Within this scheme, the renormalized locator γ again contains terms of (2.2) that start and end on the same site. The approximation is, however, the lowest order in a cluster expansion, and correct averaging of only those terms that have a single-site nature (in diagrammatic language, those terms not containing crossed lines) is all that is required. Keeping (2.3) in mind, we can see that the series for $\langle G\rangle$ must have the form

$$\langle G\rangle=\gamma+\gamma t\gamma+\gamma t\gamma t\gamma+\cdots \ , \tag{2.5}$$

where the first and last γ in the second and all subsequent terms refer to different sites. This ensures that the diagonal part of $\langle G\rangle$ is just γ, and comes entirely from the first term of (2.5). A further restriction must be applied, however; viz., in any term of (2.5) none of the site indices is repeated, and thus all γ's of a particular term refer to different sites. This restriction can be

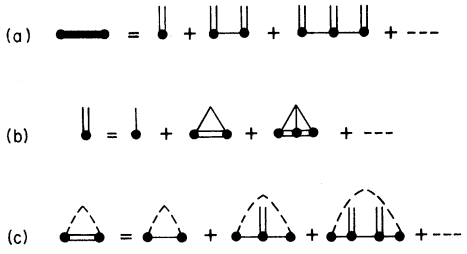

FIG. 1. Diagrams for complete Green's function (a), renormalized locator (b), and interactor (c). A restricted sum on all indices is understood unless explicitly indicated otherwise.

understood if we remember that γ has been defined so as to include properly all irreducible diagrams containing single-site scattering. The nth-order term in (2.5) then comprises all reducible diagrams containing n irreducible parts. Without the restriction on repeatability of site indices, we would obtain spurious contributions to irreducible single-site diagrams or irreducible parts of single-site diagrams.

It is straightfoward to write down a formal expression for the renormalized locator γ in terms of the restricted summation of (2.5). The difficult task then becomes the explicit summation of the restricted series. The basic trick is to relate the restricted sum to a completely unrestricted sum, which can be simply carried out in k representation. In this section we use one device for carrying out the program, and, in Appendix A, we outline an alternative procedure that some readers might find clearer.

At this point the discussion is expedited by going over to a diagrammatic development. We use the following notation: A heavy horizontal line represents the averaged Green's function in the single-site approximation; single and double vertical lines are, respectively, bare and renormalized locators; and single and double horizontal lines are, respectively, bare and renormalized interactors. The bare interactor is the hopping integral t_{ij} itself; the renormalized interactor is the appropriate sum of hopping processes.

To simplify the notation, all sites are considered inequivalent unless explicitly indicated otherwise. Also, we denote the averaged Green's function by $G[\gamma]$ (anticipating the use of functionals), without explicit need of the averaging symbol. Thus, the single-site locator expansion can be summarized by the three graphical equations of Fig. 1: (a) is the restricted series for $G[\gamma]$, viz., Eq. (2.5); (b) represents the renormalized locator; and (c) shows the diagonal element of the renormalized interactor. The broken line has no factor associated with it, and appears merely to indicate that the end-point sites are the same.

The equation for the renormalized interactor $U[\gamma]$ can be written

$$U[\gamma] = t + (tG[\gamma]t)' \quad . \tag{2.6}$$

The use of the prime in (2.6) is to indicate that internal sites must be distinct from the end-point sites which are associated with the two hopping integrals. To make this point clear, consider a typical term in the expansion of (2.6) [the next term in the series of Fig. 1(c)] for the diagonal element $U_0[\gamma]$. Such a term is shown in Fig. 2(a). In the absence of the prime the appearance of spurious terms, such as that of Fig. 2(b), would also occur. An expression that is equivalent to (2.6), but one that is much more convenient to work with, is the following:

$$U_0[\gamma] = \gamma^{-1}(G[\gamma]t)_0 \quad . \tag{2.7}$$

This is easily understood by a comparison of Figs. 1(a) and 1(c)—the addition of a t at one end of Fig. 1(a) and the dropping of a γ at the other end will give us U with the required properties.

Now, as Fig. 1(b) indicates, the renormalized locator can be written

$$\gamma = \langle g/(1 - gU_0[\gamma]) \rangle \quad , \tag{2.8}$$

where the angular brackets denote the configurational average. We are still faced, however, with the explicit summation of $G[\gamma]$. This can be accomplished by a simple functional analysis. Define the quantity Γ by

$$\Gamma = \gamma/(1 - \gamma U_0[\Gamma]) \quad . \tag{2.9}$$

Now, in Figs. 1(a) and 1(c), replace γ (double vertical lines) by the new quantity Γ. This just defines the new functional $G[\Gamma]$ which, by the definition (2.9), can be expressed in terms of γ. After a little consideration (for example, by writing out the first few diagrams—ignoring the contribution of crossed-line diagrams) one discovers that the resulting series in γ is just the same as the series for $G[\gamma]$—but with the summation restriction removed. This sum is easily performed in the k representation to give

$$G_k[\Gamma] = \gamma/(1 - \gamma t_k) \quad , \tag{2.10}$$

where t_k is the bare interactor t in the k representation. Hence, rearranging (2.9),

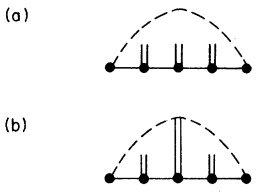

FIG. 2. Example of an allowed diagram (a) and a forbidden diagram (b) and an illustration of the need for the prime in Eq. (2.6).

$$\gamma = \Gamma/(1+U_0[\Gamma]\Gamma)\ , \tag{2.11}$$

and substituting for γ in (2.10), we have

$$G_k[\Gamma] = \frac{\Gamma}{1+\Gamma(U_0[\Gamma]-t_k)}\ . \tag{2.12}$$

The right-hand side of (2.12) is now expressed entirely in terms of the argument of the functional G_k. Thus it is now trivial to write the desired quantity $G_k[\gamma]$ as

$$G_k[\gamma] = \frac{\gamma}{1+\gamma(U_0[\gamma]-t_k)}\ . \tag{2.13}$$

Since

$$\gamma = (1/N)\sum_k G_k[\gamma] = G_0\ ,$$

Eqs. (2.7), (2.8), and (2.13) constitute a self-consistent solution within the single-site approximation.

For example, if we choose a crystal with localized energy levels of zero as the "unperturbed" lattice (we could equally well choose the pure-A or pure-B lattice), we can write

$$G_k = 1/(E-\Sigma-t_k)\ , \tag{2.14}$$

which, from (2.13), identifies the self-energy Σ as

$$\Sigma = E-(\gamma^{-1}+U_0)\ . \tag{2.15}$$

Then using (2.15) to replace U_0 in (2.8), one gets, in a few simple steps, the equation

$$\Sigma = \bar{\epsilon}-(E_A-\Sigma)G_0(E_B-\Sigma)\ , \tag{2.16}$$

where $\bar{\epsilon}$ is the virtual crystal energy $c_A E_B + c_B E_B$, and c_A and c_B are the concentrations of A and B components, respectively. Equation (2.16) is just the usual result for the CPA.[3,4]

To compare the above development with Leath's, we point out that in his work[12] the renormalized locator (there called σ) is defined with respect to an unrestricted Green's-function sum. The starting point is now an expansion such as our Eq. (2.5) or Fig. 1(a) [and Fig. 1(c) for the renormalized interactor], but without the restriction on repeated site indices. It is then necessary to make multiple-occupancy corrections to the locator itself by the subtraction of appropriate sets of diagrams from a basic locator defined similarly to our Fig. 1(b).

That the two approaches are equivalent is clear; they are both single-site approximations and thus give the same averaged Green's function. They do differ, however, in their definition of a renormalized locator; e.g., Eq. (2.3) does not hold in Leath's procedure. Our treatment, in fact, involves a simple expression for the renormalized locator—although, of course, at the cost of having to evaluate a restricted sum.

As will be shown in Sec. III, the use of the above-defined renormalized locator (without the need for explicit multiple-occupancy corrections) plays an important role in the ensuing development. We now turn to the problem of generalizing these results to a compositionally dependent hopping integral.

III. "LOCATOR-MATRIX" APPROACH TO GENERAL RANDOMNESS

The work of Leath[12] has demonstrated that, for randomness in the diagonal part of the Hamiltonian only, the propagator and locator techniques provide entirely equivalent ways of treating the averaged alloy problem; there is no reason for preferring one approach over the other. In this section we will show how, by use of the locator formalism, off-diagonal randomness may be introduced into the problem in a very natural way. The basic philosophy is, if the very useful CPA result can be obtained in terms of delocalization of atomic states by a fixed hopping integral, then it should be meaningful to generalize this physical concept by allowing delocalization to take place via a random hopping integral. Let us consider a very simple method of setting up the problem.

We first have to generalize the Hamiltonian (2.1) such that t is random. The following notation is used:

$$\begin{aligned} t_{ij} &= \alpha_{ij} \text{ if sites } i,\ j \text{ are of type } A \\ &= \beta_{ij} \text{ if they are of type } B \\ &= \zeta_{ij} \text{ if one is an } A \text{ site and the other, } B. \end{aligned} \tag{3.1}$$

Now introduce occupation indices x_i and y_i such that

$$\begin{aligned} &x_i = 1,\ y_i = 0 \text{ if } i \text{ is an } A \text{ site}\ , \\ &x_i = 0,\ y_i = 1 \text{ if } i \text{ is a } B \text{ site.} \end{aligned} \tag{3.2}$$

The following are some examples of their properties:

$$\begin{aligned} &x_i y_i = 0, \qquad x_i^2 = x_i\ , \\ &\langle x_i\rangle = c_A, \quad \langle y_i\rangle = c_B\ . \end{aligned} \tag{3.3}$$

c_A and c_B are the concentrations of A and B components, respectively. As in Sec. II, the bare locator is denoted by g_l and can take the values $(E-E_A)^{-1}$ or $(E-E_B)^{-1}$. As a locator development, the alloy Green's function appropriate for the generalization of (3.1) can be written

$$G_{ll'} = g_l\delta_{ll'} + g_l[x_l\alpha_{lm}x_m + y_l\beta_{lm}y_m + x_l\zeta_{lm}y_m + y_l\zeta_{lm}x_m]G_{ml'}\ . \tag{3.4}$$

Notice that all the randomness is now associated with a single site (it occurs in g, x, and y only) rather than with pairs of sites as well. This sim-

plification[24] greatly facilitates subsequent development.

Now, keeping in mind the properties of the occupation indices [as in relations (3.3)], let us pre- and postmultiply (3.4) by the various combinations of the pair $\{x, y\}$. Four equations are obtained,

$$\begin{aligned} x_l G_{ll'} x_{l'} &= x_l g_l \delta_{ll'} + x_l g_l \alpha_{lm} x_m G_{ml'} x_{l'} + x_l g_l \zeta_{lm} y_m G_{ml'} x_{l'} , \\ y_l G_{ll'} y_{l'} &= y_l g_l \delta_{ll'} + y_l g_l \beta_{lm} y_m G_{ml'} y_{l'} + y_l g_l \zeta_{lm} x_m G_{ml'} y_{l'} , \\ x_l G_{ll'} y_{l'} &= x_l g_l \alpha_{lm} x_m G_{ml'} y_{l'} + x_l g_l \zeta_{lm} y_m G_{ml'} y_{l'} , \\ y_l G_{ll'} x_{l'} &= y_l g_l \beta_{lm} y_m G_{ml'} x_{l'} + y_l g_l \zeta_{lm} x_m G_{ml'} x_{l'} . \end{aligned} \tag{3.5}$$

For brevity we will write

$$\begin{aligned} &x_l G_{ll'} x_{l'} = G^{AA}_{ll'}, \quad y_l G_{ll'} y_{l'} = G^{BB}_{ll'}, \\ &x_l G_{ll'} y_{l'} = G^{AB}_{ll'}, \quad y_l G_{ll'} x_{l'} = G^{BA}_{ll'}, \\ &x_l g_l = x_l/(E - E_A) = g^A_l , \\ &y_l g_l = y_l/(E - E_B) = g^B_l \quad . \end{aligned} \tag{3.6}$$

On averaging, the weights will thus be included implicitly, e.g.,

$$\langle g^A_l \rangle = c_A/(E - E_A), \quad \langle g^B_l \rangle = c_B/(E - E_B), \tag{3.7}$$

and note also that

$$\langle (g^A_l)^2 \rangle = c_A/(E - E_A)^2 .$$

The weight is correct because of the property $x_l^2 = x_l$. The complete averages can then be obtained from the relations

$$\begin{aligned} \langle g \rangle &= \langle g^A \rangle + \langle g^B \rangle , \\ \langle G \rangle &= \langle G^{AA} \rangle + \langle G^{BB} \rangle + \langle G^{AB} \rangle + \langle G^{BA} \rangle . \end{aligned} \tag{3.8}$$

The fact that a site cannot be occupied both by an atom of type A and one of type B is clearly taken care of by the property $x_l y_l = 0$, and thus G^{AB}_{ll} must be identically zero.

Replacing (3.6) in (3.5), we can express the four equations in a convenient form as a 2×2 "locator-matrix" expansion,

$$\begin{pmatrix} G^{AA} & G^{AB} \\ G^{BA} & G^{BB} \end{pmatrix}_{ll'} = \begin{pmatrix} g^A & 0 \\ 0 & g^B \end{pmatrix}_l \delta_{ll'} + \begin{pmatrix} g^A & 0 \\ 0 & g^B \end{pmatrix}_l \begin{pmatrix} \alpha & \zeta \\ \zeta & \beta \end{pmatrix}_{lm} \times \begin{pmatrix} G^{AA} & G^{AB} \\ G^{BA} & G^{BB} \end{pmatrix}_{ml'} . \tag{3.9}$$

With the right-hand side of (3.9) expanded in a perturbation series we notice that all the randomness occurs in the g matrices only and thus, apart from the fact that matrices take the place of c numbers, we have a locator development identical in form to that of the diagonal randomness case. This fact is immediately suggestive of the means of configuration averaging. The procedure that we will use is simply that of Sec. II appropriately generalized for dealing with matrices. Although our motivation for expressing the locator expansion in this form is clearly to facilitate the averaging process, there are two other aspects of (3.9) to note. This expression is particularly convenient as it is in a form that implicitly keeps account of the allowable order of successive hopping processes through the laws of matrix multiplication. Furthermore, in processes involving repeated hoppings off the same site, the possibility of simultaneous occupancy of that site by both A and B species is precluded by the property of the occupation indices, $x_i y_i = 0$, which is implicit in a product such as $g^A_i g^B_i$.

With the following quantities understood as matrices, we rewrite (3.9) as

$$G_{ll'} = g_l \delta_{ll'} + g_l t_{lm} G_{ml'} \tag{3.10}$$

and return to the considerations of Sec. II. Before discussing the configuration averaging of (3.10), however, we will clarify a point that otherwise might appear inconsistent in the later development. Consider the averaging of the diagram of Fig. 3 which comprises just bare locators and interactors (now both 2×2 matrices). The internal part of the diagram $(tgt)_0$ is just one contribution to a renormalized interactor matrix. Let us now focus our attention on the part of this term off-diagonal in the superscripts, i.e., $(tgt)^{AB}_0$. We might expect that this term, and the off-diagonal part of the renormalized interactor matrix itself, will vanish as hopping begins and ends on the same site, but the species superscripts are different. From matrix multiplication and averaging, though, we find that

$$\langle (tgt)^{AB}_0 \rangle = (\alpha \langle g^A \rangle \zeta)_0 + (\zeta \langle g^B \rangle \beta)_0 ,$$

which is certainly not zero. However this and any other term of the off-diagonal element of the renormalized interactor matrix will never contribute to the series expansion for γ or for G. Such terms will always be associated with additional factors—in this case, $g^A (tgt)^{AB}_0 g^B$. It is these that cause the contribution to vanish because of the factors $x_i y_i$ (= 0) implicit in the product $g^A g^B$. Thus our formalism is well behaved, although the occurence of a renormalized interactor, which is diagonal as regards sites and off-diagonal as regards

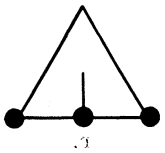

FIG. 3. A diagram that clarifies behavior of AB element of renormalized interactor.

species and yet nonzero, may be at first be a little surprising.

We will now proceed with the configuration averaging of (3.10) Very little change is needed in the discussion of Sec. II except for reciprocals being replaced by matrix inverses. The renormalized locators and interactors are now matrices, while the number unity becomes the unit matrix. Equation (2.7) remains the same,

$$U_0[\gamma] = \gamma^{-1}(G[\gamma]t)_0 , \tag{3.11}$$

and (2.8) becomes simply

$$\gamma = \langle g(1 - U_0[\gamma]g)^{-1}\rangle . \tag{3.12}$$

The matrix generalizations of the steps leading to the alloy Green's function can be written down term by term in analogy to the discussion of Sec. II. The final result, however, is immediately available by inspection of (2.13),

$$G_k[\gamma] = [1 + \gamma(U_0[\gamma] - t_k)]^{-1}\gamma . \tag{3.13}$$

This completes our formal generalizations of the alloy problem. The remainder of this section will be devoted to expressing our theory in a form that is more convenient and in which the physical content is more transparent.

When we need to refer to the specific matrix elements of U_0, we will use the notation

$$U_0 = \begin{pmatrix} U_1 & U_3 \\ U_3 & U_2 \end{pmatrix} . \tag{3.14}$$

The averaging in (3.12) can be done in a straightfoward manner, giving the result

$$\gamma = \begin{pmatrix} \gamma^A & 0 \\ 0 & \gamma^B \end{pmatrix} , \quad \gamma^A = \frac{c_A}{E - E_A - U_1} , \quad \gamma^B = \frac{c_B}{E - E_B - U_2} . \tag{3.15}$$

From (3.15) it is seen that a new feature of our theory is the association of differently renormalized locators, appropriately weighted, with each of the atomic species. This feature of the present approach is very appealing to physical intuition. Because of the randomness in the hopping integral the manner in which an electron diffuses away from a given site will be dependent on the atomic species occupying that site. Thus we can realize the desirability of retaining some distinction between species throughout the averaging process. The inherent nonequivalence of atomic type, even on averaging, is reflected in the self-energy corrections of the renormalized locators in (3.15); U_1 and U_2 are generally unequal. In the standard CPA, where the hopping integral is assumed nonrandom, U_1 becomes equal to U_2, and the necessity for distinguishing between atomic species throughout averaging no longer applies. This simply emphasizes the fact that only in that particular limit do both A and B atoms "see" the same effective environment and interact with it in the same way. From the above discussion it can be seen that the locator language provides a very natural description of the generalized alloy model. Our insistence on the simpler definition of a renormalized locator in the discussion of Sec. II now becomes clear.

Let us now turn to the complete Green's function of (3.13). Replacement of γ from (3.15) provides us with the relation

$$G_k = \begin{pmatrix} B - \beta_k & \zeta_k - U_3 \\ \zeta_k - U_3 & A - \alpha_k \end{pmatrix} \Big/ D_k , \tag{3.16}$$

where the denominator D_k is given by

$$D_k = (AB - U_3^2) - (A\beta_k + B\alpha_k - 2U_3\zeta_k) + (\alpha_k\beta_k - \zeta_k^2) , \tag{3.17}$$

and, for compactness, we have written

$$A = U_1 + 1/\gamma^A , \quad B = U_2 + 1/\gamma^B . \tag{3.18}$$

By invoking (3.15) we can eliminate U_1 and U_2 to give

$$A = (E - E_A) + c_B/\gamma^A , \quad B = (E - E_B) + c_A/\gamma^B . \tag{3.19}$$

For completeness we include here our yet unused relation (3.11). The alloy Green's function G is replaced by its value from (3.16) to give

$$\begin{pmatrix} \gamma^A U_1 & \gamma^A U_3 \\ \gamma^B U_3 & \gamma^B U_2 \end{pmatrix} = \frac{1}{N}\sum_k \begin{pmatrix} B\alpha_k - U_3\zeta_k + \zeta_k^2 - \alpha_k\beta_k & B\zeta_k - U_3\beta_k \\ A\zeta_k - U_3\alpha_k & A\beta_k - U_3\zeta_k + \zeta_k^2 - \alpha_k\beta_k \end{pmatrix} \Big/ D_k . \tag{3.20}$$

With the help of the definitions (3.18), we confirm from (3.20) the relations

$$G_0^{AA} = \gamma^A , \quad G_0^{BB} = \gamma^B , \quad G_0^{BA} = G_0^{AB} = 0, \tag{3.21}$$

which are, of course, necessary for internal consistency in this treatment. In fact, if we assume these relations, which we are certainly entitled to do as they are inherent in our averaging procedure, the system of equations (3.16) can be solved without the explicit use of (3.11). Equation (3.20) will be useful, however, for the dis-

cussion of Sec. IV.

If we perform a summation over k states in (3.16) and use the relations (3.21), we obtain three self-consistent equations,

$$\gamma^A = (1/N)\sum_k (B-\beta_k)/D_k\,,$$
$$\gamma^B = (1/N)\sum_k (A-\alpha_k)/D_k\,, \qquad (3.22)$$
$$0 = (1/N)\sum_k (\zeta_k - U_3)/D_k\,.$$

D_k is substituted in from (3.17) and then A and B can be eliminated by use of (3.19). We thus have three equations which must be solved simultaneously in order to determine the two renormalized locators γ^A and γ^B and the renormalized interactor U_3. Equations (3.22) represent, then, our approach to the generalized alloy problem, and replace the single self-consistent equation of the standard CPA. Before proceeding further we will make the connection to the CPA by examining the behavior of the expressions derived in this section in the limit of nonrandom hopping ($\alpha=\beta=\zeta$).

IV. STANDARD CPA LIMIT

The first simplification that occurs in the limit $\alpha_k=\beta_k=\zeta_k$ ($=t_k$) is an equality in all the elements of the renormalized interactor, i.e., $U_1=U_2=U_3$ ($=U$, say). This is most easily seen by a comparison of the pair of elements in the top row of (3.20). This gives us $U_1=U_3$; the pair in the bottom row then gives us $U_2=U_3$. Bearing in mind the relation (3.8), the addition of the four elements of (3.16) gives us the total alloy Green's function

$$G_k = \left(\frac{AB-U_3^2}{A+B-2U_3} - t_k\right)^{-1}\,. \qquad (4.1)$$

A self-energy is defined in the usual way,

$$G_k = (E-\Sigma-t_k)^{-1}\,, \qquad (4.2)$$

which, by a comparison with (4.1), the equality of the U's, and the definition of A and B of (3.18), allows us to write

$$E-\Sigma = U+(\gamma^A+\gamma^B)^{-1}. \qquad (4.3)$$

Now, by the use of Eqs. (3.15) and remembering that $\gamma^A+\gamma^B=G_0$, we are able to obtain after a little manipulation the relation

$$\Sigma = \bar{\epsilon} - (E_A-\Sigma)G_0(E_B-\Sigma)\,, \qquad (4.4)$$

where $\bar{\epsilon}$ is the virtual crystal energy. Referring back to (2.16), we see that (4.4) is the usual CPA self-energy equation. Having established the correct limiting behavior, we now return to the general case.

V. NUMERICAL RESULTS

Our set of self-consistent equations are applicable quite generally, but, for numerical calculations, a model of nearest-neighbor hopping provides us with useful simplifications. We will proceed with this restriction and write

$$\alpha_k=\lambda W_k\,,\quad \beta_k=\mu W_k\,,\quad \zeta_k=\nu W_k\,, \qquad (5.1)$$

where W_k is an appropriate structure factor. Introducing now Ψ and Φ defined by

$$\Psi=(1/N)\sum_k D_k^{-1}\,,\quad \Phi=(1/N)\sum_k W_k D_k^{-1} \qquad (5.2)$$

we can rewrite Eqs. (3.22) in a useful form,

$$\gamma^A = B\Psi-\mu\Phi\,,\quad \gamma^B = A\Psi-\lambda\Phi\,,\quad 0=U_3\Psi-\nu\Phi. \qquad (5.3)$$

Eliminating Ψ and Φ from (5.3) gives us the relation

$$U_3 = \frac{\nu(A\gamma^A-B\gamma^B)}{(\lambda\gamma^A-\mu\gamma^B)}\,, \qquad (5.4)$$

thus reducing the number of equations in which a k summation is needed from three to two, viz., those for the two locators

$$\gamma^A = \frac{1}{N}\sum_k \frac{B-\mu W_k}{p-qW_k+rW_k^2}\,,$$
$$\gamma^B = \frac{1}{N}\sum_k \frac{A-\lambda W_k}{p-qW_k+rW_k^2}\,, \qquad (5.5)$$

where

$$p=AB-U_3^2\,,\quad q=A\mu+B\lambda-2U_3\nu\,,\quad r=\lambda\mu-\nu^2\,. \qquad (5.6)$$

At this stage we have simplified our expressions as far as is possible and so turn to the results of numerical calculation as the most efficient way of displaying the essential features of the theory. The reader is referred to Appendix B for details of the actual calculation of the locators of (5.5). Suffice it to mention here that the structure factor used was one appropriate to a simple cubic lattice (of nearest-neighbor distance a) with a half-bandwidth of unity, viz.,

$$W_k = \tfrac{1}{3}(\cos k_x a+\cos k_y a+\cos k_z a). \qquad (5.7)$$

The quantities calculated are those of immediate physical interest: the total and partial alloy densities of states

$$\rho_{A,B} = -(1/\pi)\,\mathrm{Im}\,\gamma^{A,B}\,,\quad \rho_{\mathrm{tot}}=\rho_A+\rho_B\,. \qquad (5.8)$$

A fairly comprehensive set of figures is given and so a brief summary of their content should be helpful. The bulk of the discusison will center on Figs. 4–9, which all pertain to the same set of alloy compositions. The principal quantity of interest is the total alloy density of states ρ_{tot}, which is plotted in Fig. 4 for $c_A=0.6$, $c_B=0.4$, $E_A=-E_B=0.2$, $\nu=1$, and for various values of λ and μ. For economy of presentation we have taken $\nu=\frac{1}{2}(\lambda+\mu)$, a choice which is physically reasonable, but not at all essential to the development of the theory or to the mechanics of the numerical analysis. The

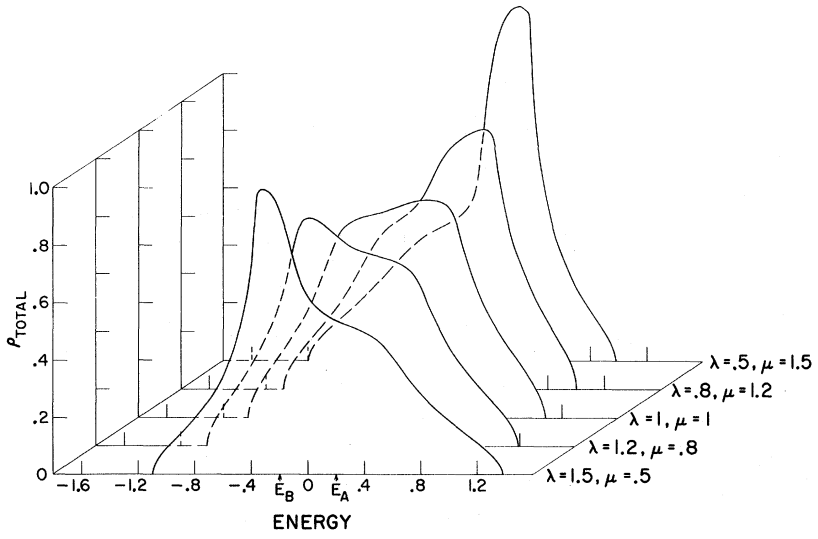

FIG. 4. Total density of states for five different alloys. $E_A = -E_B = 0.2$, $c_A = 0.6$, $c_B = 0.4$, and the A-B hopping (ν) is 1.0. The A-A (λ) and B-B (μ) hoppings are indicated at the right of the figure.

case $\lambda = \mu = 1$ gives the standard CPA result and is displayed in the central curve of the figure. In Figs. 5 and 6 we show the separate component densities of states ρ_B and ρ_A, respectively. The concentration weighting is, of course, included as it is inherent in the definitions. These quantities, when integrated over the occupied portion of the band, indicate how, on average, the charge density per atom is distributed between the two constituent atomic species. The real parts of γ^A and γ^B are shown in Figs. 7 and 8, respectively, while in Fig. 9 the real part of G_0 ($= \gamma^A + \gamma^B$) is given. In these last three curves we have omitted the plots for the alloys with $\lambda = 1.2$, $\mu = 0.8$ and $\lambda = 0.8$, $\mu = 1.2$ for clarity of display. In Fig. 10 we again show a density-of-states plot. Here the relative concentrations are changed to $c_A = 0.9$ and $c_B = 0.1$, but otherwise the parameters are the same as in Fig. 4. Two examples of the split-band regime are displayed in Figs. 11 and 12. In the former we have $E_A = -E_B = 0.75$, $c_A = 0.6$, $c_B = 0.4$, and $\nu = 1$; in the latter we have just changed the concentrations to $c_A = 0.9$, $c_B = 0.1$. Finally, in Figs. 13 and 14 we show the effects of changing ν for fixed values of λ and μ. In Fig. 13 the total density of states is plotted, and in Fig. 14 the component densities are given. In both figures the parameters are $E_A = -E_B = 0.2$, $c_A = 0.6$, $c_B = 0.4$, $\lambda = 0.8$, and $\mu = 1.2$.

We now discuss the features of the theory in some detail and return to the total density-of-states curves of Fig. 4. The front curve of the set illustrates the ρ_{tot} of an alloy for which the pure host (A) band is three times wider than, and completely overlaps, the pure solute (B) band. As we move back through the set of curves, the host band narrows while the solute band broadens until, finally, the host band is one-third the width of, and completely overlapped by, the band of the pure solute. In each case, the host band is centered above the solute band center. The rather marked effects of the different constituent bandwidths are clearly evident in the figure and are, of course, very much as one would expect. In the first curve ($\lambda = 1.5$, $\mu = 0.5$), for example, the influence of the much narrower solute (B) band shows up dramatically in the negative-energy portion of the spectrum. A comparison with Fig. 5 shows that most of the weight in this negative-energy ($E \simeq -0.3$) peak is contributed by the B component density ρ_B. Interestingly, however, ρ_A (cf. Fig. 6) also exhibits a small "satellite" peak in the same region. This extra structure can be seen in the same energy

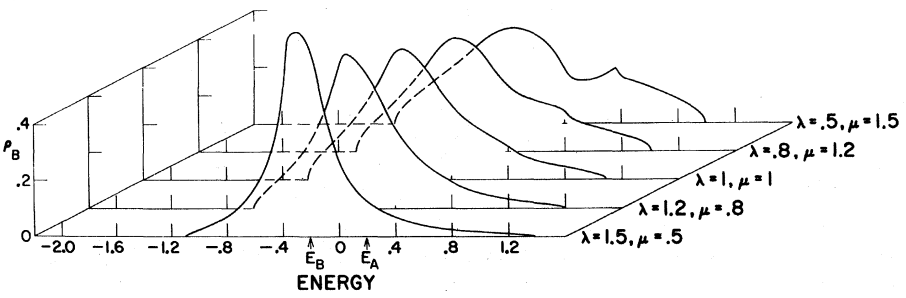

FIG. 5. B (minority) component density of states (ρ_B) for the alloys of Fig. 4.

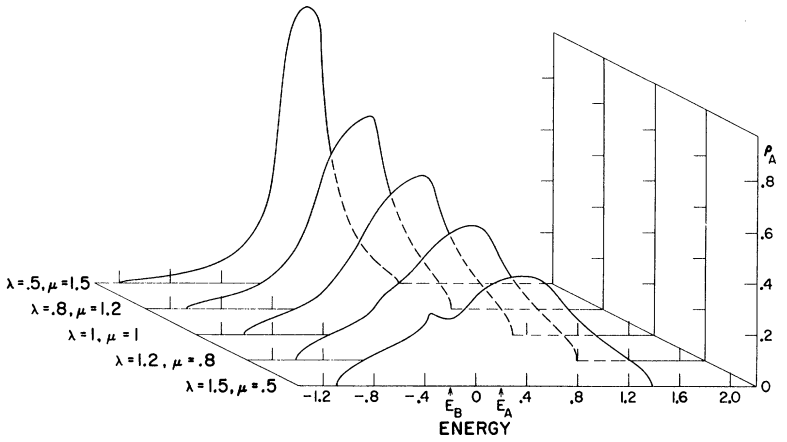

FIG. 6. A (majority) component density of states (ρ_A) for the alloys of Fig. 4.

region of the corresponding curve in Fig. 7 for the real part of γ^A. The satellite peak in ρ_A is evidently a reflection of the fact that the density of states of the much narrower pure B band varies strongly with energy in a region accessible to the wide pure A spectrum. Since the renormalization of the locator associated with the A species is due to the replacement of A atoms by B atoms, and is energy dependent. it is sensitive to the piling up of B-like states in the negative-energy portion of the spectrum. One sees no corresponding satellite structure in the positive-energy tail of the rather featureless ρ_B. This is consistent with our interpretation, since the A band density of states does not vary sufficiently rapidly on the scale of the width of the B band. On the other hand, for $\lambda = 0.5$ and $\mu = 1.5$, the host band is much narrower and, indeed, contributes structure to the positive-energy portion of ρ_B. It is, in fact, somewhat enhanced in this case because of the higher concentration of A atoms. As the other curves in Figs. 5 and 6 indicate, this satellite effect depends rather sensitively on one of the constituent bands being sufficiently narrow compared to the other. The development of satellite structure in the component densities of states can be physically important. For

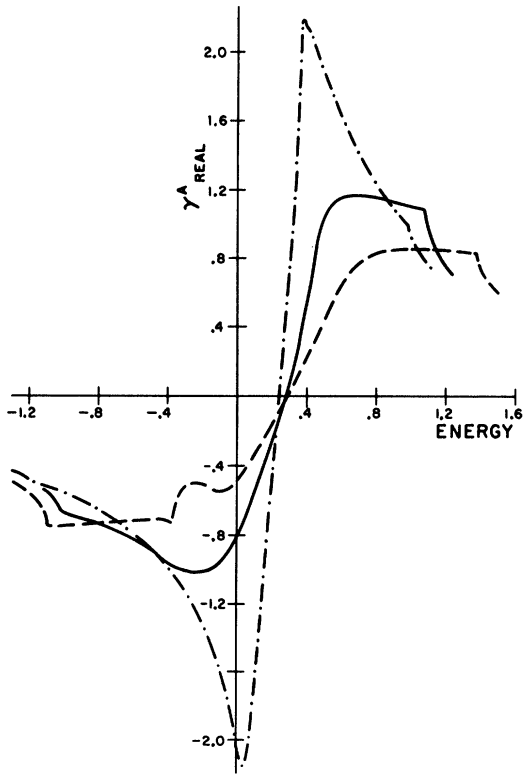

FIG. 7. Real part of renormalized locator γ^A for three of the alloys of Fig. 4. Solid curve, $\lambda=\mu=1.0$; dashed curve, $\lambda=1.5$, $\mu=0.5$; dot-dashed curve, $\lambda=0.5$, $\mu=1.5$.

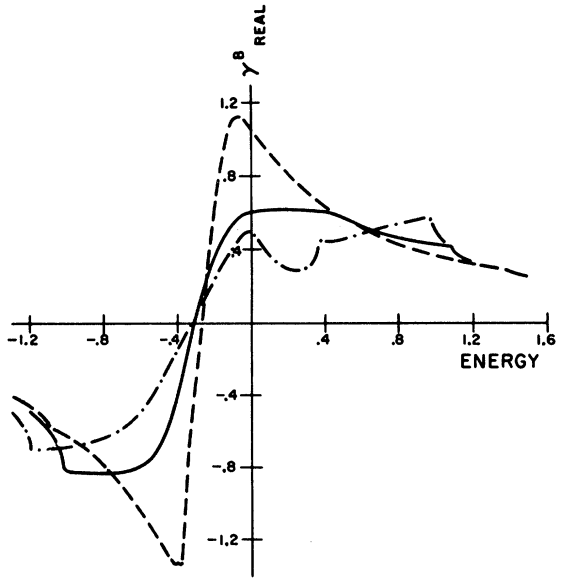

FIG. 8. Real part of renormalized locator γ^B. Notation is that of Fig. 7.

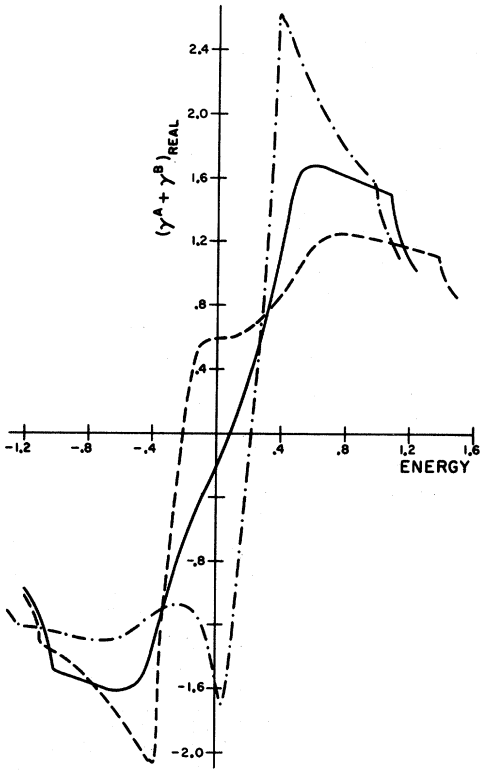

FIG. 9. Real part of total Green's function G_0 $(=\gamma^A+\gamma^B)$.

example, referring again to the case of $\lambda = 1.5$ and $\mu = 0.5$, the existence of a negative-energy peak in ρ_A suggests that, on the average, slightly more charge is concentrated about the A-type constituent (and slightly less about the B type) than would be inferred if the weight of the peak in ρ_{tot} were attributed solely to a peak in ρ_B.

The set of alloys, whose densities of states are illustrated in Fig. 10, corresponds to those of Fig. 4, but with $c_A = 0.9$ and $c_B = 0.1$. The same trends are evident, but less strikingly because of the smaller concentration of B atoms. Note that, while the curve for $\lambda = 0.5$, $\mu = 1.5$ is essentially A-like in the upper portion of the band, it falls off too rapidly in the lower portion; the lower band edge comes at about $E = -0.2$, which corresponds to the center of the pure B band. Despite the small concentration of B atoms, energies below the indicated band edge should be accessible in a long B-like "tail" of the density of states. Such tailing, however, is not properly dealt with in a single-site approximation, and one can expect that the neglect of cluster effects will become a more severe approximation in such an energy region when the constituent bandwidths differ considerably from each other.

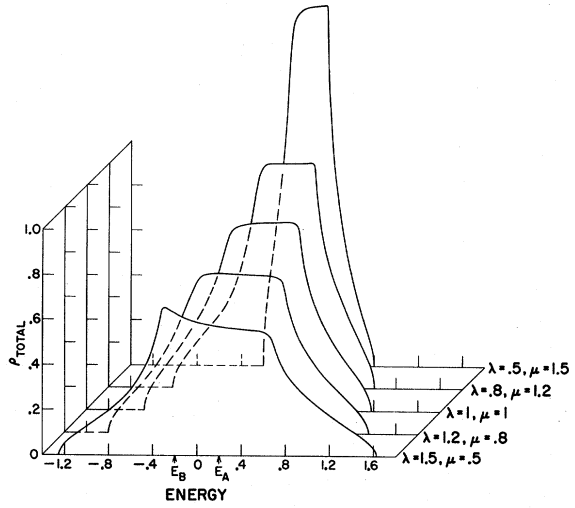

FIG. 10. Total density of states for the parameters $E_A = -E_B = 0.2$, $c_A = 0.9$, $c_B = 0.1$, and $\nu = 1.0$.

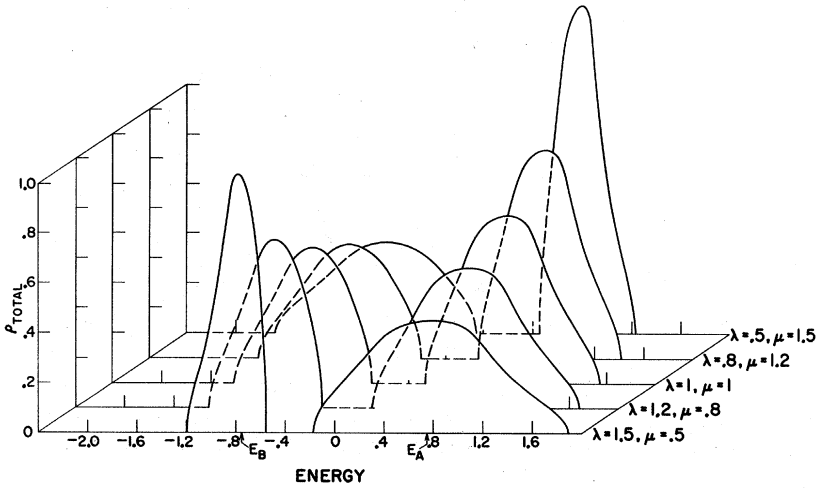

FIG. 11. Split-band regime. The parameters are $E_A = -E_B = 0.75$, $c_A = 0.6$, $c_B = 0.4$, $\nu = 1.0$.

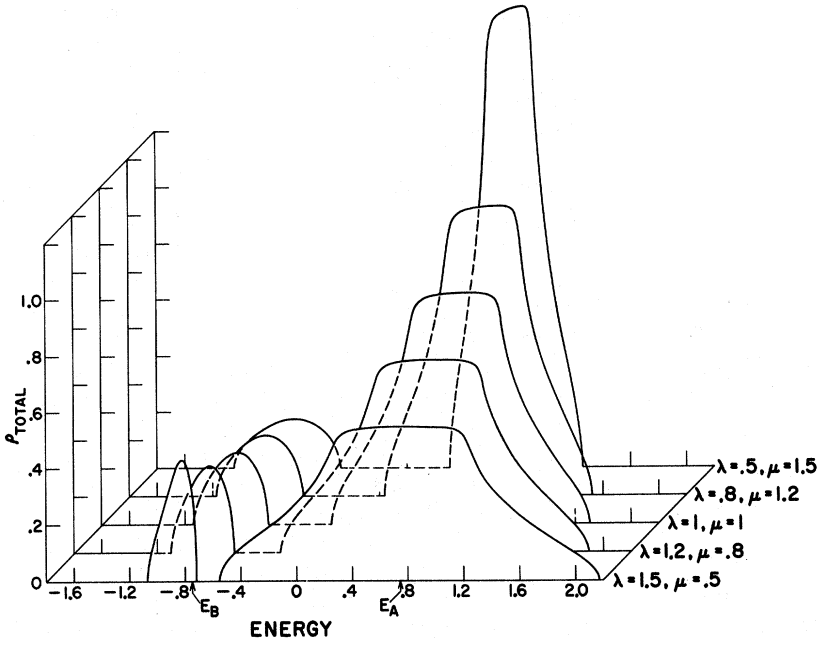

FIG. 12. As in Fig. 11, but for a different composition: $c_A = 0.9$, $c_B = 0.1$.

Two examples of the split-band regime are shown in Figs. 11 and 12. In each case $E_A = -E_B = 0.75$ and $\nu = 1$. The same set of values of λ and μ are used as in the earlier diagrams. In Fig. 11 the concentrations of the two components are $c_A = 0.6$ and $c_B = 0.4$, and in Fig. 12 $c_A = 0.9$ and $c_B = 0.1$. The behavior of the density of states, as we broaden or narrow component bands, is as expected and follows the lines of our earlier discussion. The situation is somewhat simplified here, of course, as the predominant contribution to the upper sub-band comes from ρ_A, and to the lower sub-band from ρ_B.

In all of the alloys thus far discussed, ν has been the arithmetic mean of λ and μ. In order to check that this particular choice of parameters does not bias our results in any special way, we have repeated one of the computations ($E_A = -E_B = 0.2$, $c_A = 0.6$, $c_B = 0.4$, $\lambda = 0.8$, $\mu = 1.2$) for different values of ν. The results are shown for the total and component densities of states in Figs. 13 and 14, respectively. As the changes we have chosen for ν are only small, the difference between the curves is quite minor. There is some smoothing out of the left-hand side of ρ_{tot} (Fig. 13) as we vary ν from 1.1 to 0.9; the alloy bandwidth (both figures) increases somewhat with an increased ν while, at the same time, the peaks of ρ_A and ρ_B (Fig. 14) become slightly narrowed. This completes our discussion of numerical results and we turn now to considerations of some analytic prop-

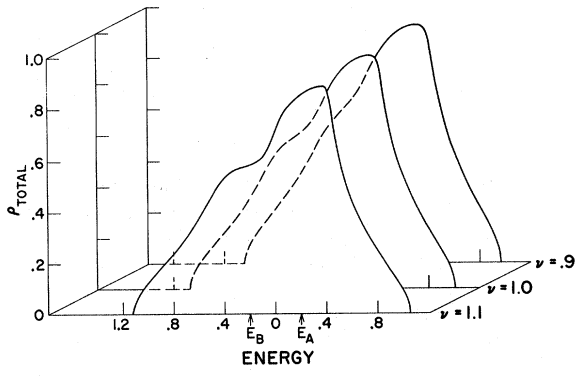

FIG. 13. Changes in ν. Here $E_A = -E_B = 0.2$, $c_A = 0.6$, $c_B = 0.4$, $\lambda = 0.8$, $\mu = 1.2$. Values of ν are shown at the right of the figure.

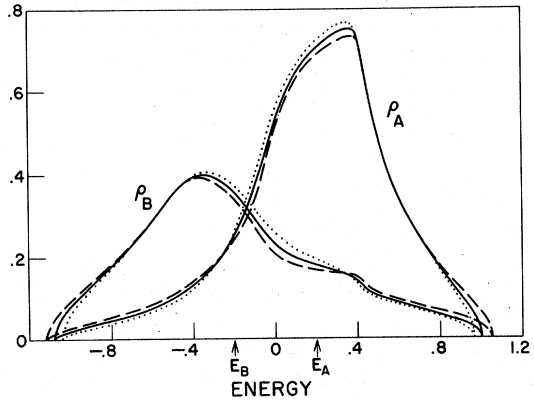

FIG. 14. Component densities of states for alloys of Fig. 13. Solid curve, $\nu = 1.0$; dashed curve, $\nu = 1.1$; dotted curve, $\nu = 0.9$.

erties of the theory.

VI. SOME FURTHER ASPECTS OF THE THEORY

In this section we complete our discussion of the theory with a brief account of a few of its general properties. Of most interest, probably, are its moment-preserving properties. We could, of course, obtain these by means of direct calculation; it is, however, considerably less arduous to use diagrammatic arguments. As such considerations involve some subtlety, it is convenient to introduce them with reference to the standard CPA—this we do in Sec. VI A—after which they are applied to the random-hopping-integral problem of the present paper.

A. Moments in CPA

According to Velický *et al.*,[4] in their work on the fixed-hopping-integral problem, the CPA preserves the first six moments, at least, of the density of states and the spectral density. This, of course, compares excellently with the figure of 3, which was the highest number preserved in earlier approaches. Whether the CPA itself preserves more than six moments is a question that, as yet, does not seem to have been answered. We will address ourselves here to that problem by way of diagrammatic considerations.

Following Velický *et al.*, we will denote the pth moment of the spectral density and the density of states by M_p and μ_p, respectively. M_p and μ_p are the coefficients in an expansion in powers of z^{-1} of the alloy Green's function $G_k(z)$ and the density of states $\rho(z)$. z is the generalized energy and, specifically, the pth moment is the coefficient of the term in $z^{-(p+1)}$.

In a diagrammatic expansion of G—we will consider "bare" diagrams for simplicity—each interactor is z independent (it is just the hopping integral), and each locator contributes to $O(z^{-1})$. Thus a diagram containing n locator lines is $O(z^{-n})$ and so may contribute to the $(n-1)$th moment (and, of course, higher-order moments as well). We may expect, therefore, that if a diagram containing n locator lines has not been averaged properly, the $(n-1)$th moment will be in error. Let us consider this in more detail both from a propagator point of view (which is simpler) and from a locator point of view.

Figures 15(a) and (b) and Figs. 15(c) and (d) represent, respectively, in the propagator and locator formalisms, the two lowest-order diagrams that the CPA does not include in a properly averaged fashion (they are all two-site cluster diagrams). The notation of the locator diagrams has been explained earlier. In the propagator diagrams, the horizontal lines are bare propagators, while the vertical lines represent scattering at impurity sites. In all cases scattering or hopping off identical sites is denoted by the joining of vertical lines. For a diagram to contribute to the density of states, it must be diagonal (initial and final sites the same); a diagram that contributes to $G_k(z)$ can, of course, be diagonal or off-diagonal.

Let us first consider the propagator diagram of Fig. 15(a). Now a single propagator is $O(z^{-1})$, but the z^{-1} term itself is diagonal (consider the expansion of a single propagator in powers of z^{-1}). Thus the leading off-diagonal contribution [which is what is required for an internal propagator of Fig. 15(a)] is $O(z^{-2})$. Hence the three internal propagators contribute to $O(z^{-6})$. The two external propagators now contribute to $O(z^{-2})$. In this order, however, the whole diagram is nondiagonal—to make it diagonal we require another power of z^{-1}. Thus the contribution of this diagram is of $O(z^{-8})$ in the off-diagonal case and $O(z^{-9})$ in the diagonal case. In terms of moments, the incorrect averaging of this diagram causes error in M_7 and μ_8. By a similar argument errors begin to arise, due to Fig. 15(b), at M_{10} and μ_9. Thus, it appears from these considerations that the CPA is correct for all moments up to M_6 and μ_7.

It will be instructive now to check out these arguments by reference to the locator diagrams. Clearly Fig. 15(c) is essentially off-diagonal (and will affect only the spectral density), while Fig. 15(d) is diagonal (and will affect both the spectral density and density of states). Referring to Fig. 15(c), it would appear, at first sight, that this diagram will give rise to error at $O(z^{-4})$, since each locator line is of $O(z^{-1})$. That this is not so can be understood from a more careful consideration of averaging in the single-site approximation. Taking just one of the pairs of locator lines in Fig. 15(c), it is clearly correctly averaged as $\langle g^2 \rangle$. However, in the single-site approximation, the pair is incorrectly weighted as $\langle g \rangle^2$; this is the weighting the members of the pair would have in the corre-

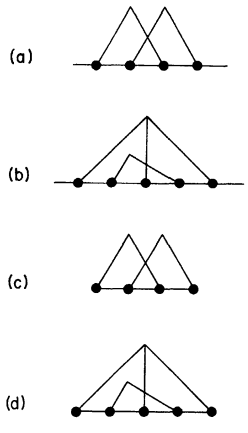

FIG. 15. Propagator diagrams [(a), (b)] and locator diagrams [(c), (d)]. These are the lowest-order diagrams that receive an incorrect weighting in the single-site approximation.

sponding single-site diagram obtained by breaking the pair (associating the two locators with different sites). Thus the correction that is required is a second-order cumulant, viz., $\langle g^2\rangle - \langle g\rangle^2$, and this is easily shown to be $O(z^{-4})$. By a consideration of all four locator diagrams (there are only three that have a single-site nature since $t_0 = 0$), it is fairly easy to see that the error produced by the incorrect averaging of the whole diagram of Fig. 15(c) is proportional to $(\langle g^2\rangle - \langle g\rangle^2)^2$. This factor is $O(z^{-8})$, which agrees with our earlier propagator argument.

We can understand this result in another way by starting with a z^{-1} expansion of the locator g. The first term in the expansion is just z^{-1} and contains no randomness; randomness, and hence the source of error in averaging, does not appear until the z^{-2} term. Thus randomness in all four locator lines, which is what is required to give the character of a crossed-line diagram, first occurs at $O(z^{-8})$, giving us the order of the error. Although one should not be too cavalier about applying such a discussion to other diagrams such as Fig. 15(d), which involve three locators associated with a single site, it is fairly easy to develop the argument in a rigorous fashion such that it can be used quite generally.

Let us now turn to Fig. 15(d) and the moments of the density of states. There are three single-site type of diagrams which contain five locators and hence are related to the diagram of the figure. By a consideration of these diagrams, it is straightforward to show that the averaging error associated with Fig. 15(d) is proportional to $(\langle g^3\rangle - \langle g^2\rangle\langle g\rangle) \times (\langle g^2\rangle - \langle g\rangle^2)$. The first factor, which is associated with the triplet of lines, is $O(z^{-5})$; the second factor, associated with the pair, is $O(z^{-4})$. Hence the whole diagram is incorrectly averaged at $O(z^{-9})$—again in agreement with the propagator argument.

In conclusion, then, the CPA preserves the first seven moments (M_0 to M_6) of the spectral density, and the first eight moments (μ_0 to μ_7) of the density of states. We will now try to extend these diagrammatic arguments to the generalized theory of this paper.

B. Moment Preservation for Random Hopping Integral

The arguments of Sec. VI A can very easily be extended to the case of a random hopping integral. Again it is Figs. 15(c) and 15(d) that we have to consider, but now the vertical and horizontal lines represent 2×2 locator and interactor matrices, respectively. To ensure that the randomness still has a single-site form, we introduced occupation indices and included them in the definition of the locator. To see the effect of this device on the moments, one has only to expand the 2×2 locator in powers of z^{-1}. Because of the presence of the occupation indices, the locator has implicit randomness in the first term, i.e., $O(z^{-1})$. It is thus immediately apparent that the orders at which errors begin to appear due to single-site averaging are $O(z^{-4})$ for Fig. 15(c) and $O(z^{-5})$ for Fig. 15(d). In our generalization of the CPA, therefore, the lowest moments not treated exactly are M_3 and μ_4; i.e., our approximation preserves the first three moments (M_0 to M_2) of the spectral density, and the first four moments (μ_0 to μ_3) of the density of states. That the single-site approximation preserves fewer moments when the hopping is random is, of course, not surprising. It is, however, satisfying to note that we have more exact moments of the density of states than do other (pre-CPA) approximations for diagonal randomness only (cf. Ref. 4).

C. Independent Band Limit

A limiting case that remains to be checked is that of vanishing A-B hopping. An electron starting on an A site then can hop only to other A sites. Similarly, an electron starting on a B site must always hop to other B sites. We must, therefore, get two bands that are independent, although, of course, they can overlap one another. This situation is, in some sense, equivalent to a vacancy problem and to the extreme split-band limit of Velický *et al.*[4] Let us fix our attention on the A sub-band. As far as this sub-band is concerned, B sites are forbidden from taking part in hopping processes and are, thus, effectively vacant sites. Consider now the split-band limit; setting $E_B \to \infty$ has the effect of preventing electrons from hopping onto B sites. We would expect, therefore, that our equations for the A sub-band, in the limit $\nu \to 0$, are the same as the CPA equation in limit $E_B \to \infty$.

Let us, then, set ν equal to zero in our equations. From (5.4) it is seen that $U_3 \to 0$. The denominator in (5.5) then factors,

$$D_k = (A - \lambda W_k)(B - \mu W_k). \tag{6.1}$$

Hence from (5.5) and the definitions (3.19)

$$\gamma^A = \frac{1}{N}\sum_k \frac{1}{E - E_A + c_B/\gamma^A - \lambda W_k}\ ,$$
$$\gamma^B = \frac{1}{N}\sum_k \frac{1}{E - E_B + c_A/\gamma^B - \mu W_k}\ . \tag{6.2}$$

Clearly we now have a pair of self-consistent equations that are independent. We can, if we wish, define two k-independent self-energies

$$\Sigma_A = E_A - c_B/\gamma^A, \quad \Sigma_B = E_B - c_A/\gamma^B\ . \tag{6.3}$$

Now the CPA equation (setting the averaged t matrix equal to zero; cf. Refs. 3 and 4) may be written

$$c_A \frac{E_A - \Sigma}{1 - G_0(E_A - \Sigma)} + c_B \frac{E_B - \Sigma}{1 - G_0(E_B - \Sigma)} = 0, \tag{6.4}$$

where G and Σ are the Green's function and self-energy of the CPA, respectively. Setting $E_B \to \infty$, we obtain

$$\Sigma = E_A - c_B/G_0 , \tag{6.5}$$

which is of just the same form as the first of Eqs. (6.3), as was anticipated.

We can now check a further limiting procedure, viz., setting $\mu \to 0$. In this case the second of Eqs. (6.2) becomes

$$\gamma^B = c_B/(E - E_B) , \tag{6.6}$$

describing completely localized levels at energy E_B and with weighting c_B. With this, the satisfactory behavior of the theory in the limit of independent bands is established.

D. "Effective" Lattice and Some Concluding Remarks

In any averaging process the actual alloy is replaced by an "effective" lattice, whose nature becomes more apparent if the Green's function G_k (taken to mean $G_k^{AA} + G_k^{BB} + G_k^{AB} + G_k^{BA}$) is expressed in the form

$$G_k(E) = (E - H_{eff})^{-1} , \tag{6.7}$$

where H_{eff} is the effective-lattice Hamiltonian and generally is energy dependent. In our case, let us assume the nearest-neighbor model [Eq. (5.1)] for simplicity and then sum the four elements of the matrix (3.16). We can then make the identification

$$H_{eff} = E - \frac{p - qW_k + rW_k^2}{(A + B - 2U_3) - (\lambda + \mu - 2\nu)W_k} , \tag{6.8}$$

where all quantities have been defined earlier in the text. At present we have been unable to reduce (6.8) to a more convenient form. We note, however, from this expression, that H_{eff} can be expressed as an infinite series in powers of W_k. It will, thus, be realized that although hopping in the real lattice connects only nearest-neighbor sites, the "effective" lattice Hamiltonian of the averaged alloy connects all sites. There are exceptions to this in special cases; for example, in the CPA limit ($\lambda = \mu = \nu$) only nearest neighbors are connected and, in the case $\lambda + \mu - 2\nu = 0$, coupling exists only out to twice the lattice constant.

Generally, then, we are using a single-site approximation and obtaining an "effective" Hamiltonian that couples all sites. This provides further indication of the nature of our approximation. It will be remembered from our introductory remarks that the CPA may be regarded as a one-impurity problem in which a single real atom is placed in an effective lattice. This real atom produces, in the single-site approximation, a perturbation at the impurity site only. The solution of this one-impurity problem provides us with an equation that describes the effective lattice. The present generalization suggests that the substitution of a single real atom into the effective lattice produces a perturbation that, instead of being localized to the impurity site, extends to all neighbors. This in turn would indicate the need, in an effective medium approach, to introduce appropriate parameters not only for the hopping between effective atoms but also for the hopping between real and effective sites.

We have demonstrated in this paper how, in a very natural way, the locator formulation allows us to generalize the alloy Hamiltonian to include site dependence in the hopping integral. Physically we are observing the delocalization of electrons from A and B atomic states, and a feature of the theory is the retention of the distinction between the two species throughout the averaging process. As yet we have been unable to express our theory in the more commonly used propagator language—this may indicate that there are certain inherent advantages in a locator approach. The theory, as expressed here, is in a form that is immediately suitable for certain extensions: (i) Although we have been concerned with the electronic problem here, a lattice-dynamics problem involving force-constant changes may be treated in an exactly analogous way. (ii) The theory may easily be extended to a multicomponent alloy, e.g., for an n-component alloy our 2×2 matrices would become $n\times n$ matrices and we would have, instead of three, $\frac{1}{2}n(n+1)$ simultaneous equations to solve. (iii) Any developments of the "diagonal randomness" problem to include the effects of higher-order clusters by a multiple-scattering or hopping technique should be readily generalized in terms of our formalism.

APPENDIX A

In Sec. II the problem at hand was the explicit summation of the restricted Green's-function series of Fig. 1(a). There we showed how the introduction of a new argument into the locator functional caused the restricted series to degenerate into the completely unrestricted series (ignoring the effect of crossed-line diagrams) which is easily summed. We present here an alternative approach that does not require the use of functionals.

Again we denote the averaged Green's function of Fig. 1(a) by $G_{ll'}$. Let us also define a quantity $G^0_{ll'}$, which is the unrestricted series associated with $G_{ll'}$; i.e., $G^0_{ll'}$ is represented by Fig. 1(a) but with the removal of the restriction on repeated site indices. It is this quantity that is easily summed (in the k representation) to give

$$G^0_k = (\gamma^{-1} - t_k)^{-1} . \tag{A1}$$

It is clear that it is necessary to subtract an infinite set of terms (diagrams) from G^0 to obtain the desired Green's function G, and that this infinite set of diagrams must be expressible in a summable form to provide a useful relationship. By a systematic inspection we find that, except for crossed-line diagrams, the following relation exists:

$$G_{ll'} = G^0_{ll'} - \sum_m G^0_{lm} U_m G_{ml'} \,. \tag{A2}$$

U_m is the renormalized interactor of Fig. 1(c) here labeled explicitly for clarity. Equation (A2) has the form of a Dyson equation, except that it is constructed to subtract, rather than add, diagrams. Since U_m is independent of site index, it can be pulled out of the summation as U_0. Note that all the quantities in (A2) are functionals of γ. We have not exploited their functional dependence here, however, and so do not display it explicitly. Now going over to the k representation, we can rearrange (A2) to obtain

$$G_k = [(G^0_k)^{-1} + U_0]^{-1} \,, \tag{A3}$$

and substituting G^0_k from (A1), we obtain

$$G_k = (\gamma^{-1} + U_0 - t_k)^{-1} \,,$$

which is just Eq. (2.13).

APPENDIX B

The numerical calculations of the k sums of (5.5) are simplified by the use of the following (easily derived) relations:

$$\frac{1}{p - qW_k + rW_k^2} = \frac{1}{2r\eta_2}[F_k(\eta_1 - \eta_2) - F_k(\eta_1 + \eta_2)], \tag{B1}$$

$$F_k(z) = (z - W_k)^{-1} \,, \quad F_0(z) = (1/N)\sum_k F_k(z) \,, \tag{B2}$$

$$\eta_1 = q/2r, \qquad \eta_2 = (q^2/4r^2 - p/r)^{1/2} \,. \tag{B3}$$

Our Eqs. (5.5) can then be written (with $\eta^{\pm} = \eta_1 \pm \eta_2$)

$$\gamma^{(A,B)} = \frac{(B,A)}{2r\eta_2}[F_0(\eta^-) - F_0(\eta^+)] - \frac{(\mu,\lambda)}{2r\mu_2}[\eta^- F_0(\eta^-) - \eta^+ F_0(\eta^+)] \,. \tag{B4}$$

The reason for expressing our equations in this rather more cumbersome form is to take advantage of numerical methods available in the literature.[25,26] Well-established techniques exist for evaluating functions such as $F_0(z)$.

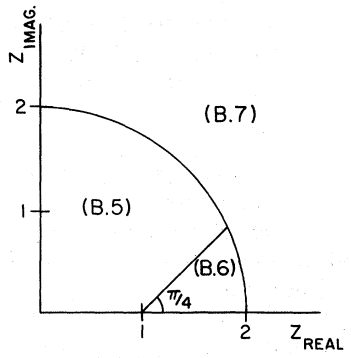

FIG. 16. Three regions of complex z plane. Figures in parentheses refer to equation numbers in the text.

The calculations were done on a CDC 6600 machine, the pair of equations (5.5)—expressed in the form (B4)—being solved for γ^A and γ^B by a Newton-Raphson technique. The procedure for calculating $F_0(z)$ will be summarized briefly here. Three expressions for it were used, the appropriate one being determined by the value of z. They are

$$F_0(z) = 3i\int_0^\infty dt\, e^{-i3zt}[J_0(t)]^3 \,, \tag{B5}$$

$$F_0(z) = 3\int_0^\infty dt\, e^{-3zt}[I_0(t)]^3 \,, \tag{B6}$$

$$F_0(z) = \frac{1}{z} + \frac{1}{6z^3} + \frac{15}{216z^5} + \frac{155}{3888z^7} + \frac{2485}{93312z^9} \,. \tag{B7}$$

The series (B7) is just the first few terms in an expansion in z^{-1} and must be the correct limit for large $|z|$; we find, in fact, that it is the best expression for $|z|$ greater than about 2. Expressions (B5) and (B6) involve Bessel functions of zero order and with real and imaginary arguments, respectively (see Wolfram and Callaway[26]). The ranges of z where each of the three expressions is used are shown in Fig. 16. We show just one quadrant—symmetry considerations determine the behavior in the other three quadrants. The figures in parentheses refer to the equation numbers. For the calculation of the integrals in (B5) and (B6) we used the Gaussian-quadrature method, based on Legendre polynomials, as described in the appendix of Hone *et al.*[25] The agreement between values of $F_0(z)$, calculated by the alternative expressions appropriate at a particular boundary of the regions in Fig. 16, was for all practical purposes exact (better than 1%). It was, in fact, with such considerations that we determined the positions of these boundaries.

*Supported by the U. S. Army Research Office, Durham, N. C.

†Present address: Department of Physics, University of Reading, Reading, England.

‡Supported in part by the Center for Theoretical Physics and in part by the U. S. Office of Naval Research.

[1]M. Lax, Rev. Mod. Phys. 23, 287 (1951).
[2]P. Soven, Phys. Rev. 156, 809 (1967).
[3]P. Soven, Phys. Rev. 178, 1136 (1969).
[4]B. Velický, S. Kirkpatrick, and H. Ehrenreich, Phys. Rev. 175, 747 (1968).
[5]P. L. Leath, Phys. Rev. 171, 725 (1968).
[6]F. Yonezawa, Progr. Theoret. Phys. (Kyoto) 40, 734 (1968).
[7]D. W. Taylor, Phys. Rev. 156, 1017 (1967).
[8]Y. Onodera and Y. Toyozawa, J. Phys. Soc. Japan 24, 1341 (1968).
[9]T. Matsubara and Y. Toyozawa, Progr. Theoret. Phys. (Kyoto) 26, 739 (1961).
[10]T. Matsubara and T. Kaneyoshi, Progr. Theoret. Phys. (Kyoto) 36, 695 (1966).
[11]J. M. Ziman, J. Phys. C 2, 1230 (1969).
[12]P. L. Leath, Phys. Rev. B 2, 3078 (1970).
[13]P. W. Anderson, Phys. Rev. 109, 1492 (1958).
[14]R. N. Aiyer, R. J. Elliott, J. A. Krumhansl, and P. L. Leath, Phys. Rev. 181, 1006 (1969).
[15]I. M. Lifshitz, Usp. Fiz. Nauk 83, 617 (1964) [Sov. Phys. Usp. 7, 549 (1965)].
[16]T. P. Eggarter and M. H. Cohen, Phys. Rev. Letters 25, 807 (1970); E. N. Economou, S. Kirkpatrick, M. H. Cohen, and T. P. Eggarter, *ibid.* 25, 520 (1970).
[17]S. Takeno, Progr. Theoret. Phys. (Kyoto) 40, 942 (1968).
[18]Y. Izyumov, Proc. Phys. Soc. (London) 87, 505 (1966).
[19]N. F. Berk, Phys. Rev. B 1, 1136 (1970).
[20]P. Soven, Phys. Rev. B 2, 4715 (1970).
[21]A preliminary report of this work appeared in Phys. Letters 35A, 205 (1971).
[22]T. Tanaka, K. Moorjani, and S. M. Bose (private communication).
[23]H. Shiba (private communication).
[24]The use of occupation indices for expressing the randomness in a single-site form has also been suggested in the work of S. F. Edwards and J. M. Loveluck, J. Phys. C 3, S261 (1970).
[25]D. Hone, H. Callen, and L. R. Walker, Phys. Rev. 144, 283 (1966).
[26]T. Wolfram and J. Callaway, Phys. Rev. 130, 2207 (1963).